GKSS
FORSCHUNGSZENTRUM
in der HELMHOLTZ-GEMEINSCHAFT

Final Draft
of the original manuscript:

Stanev, E.V.; Dobrynin, M.; Pleskachevsky, A.; Grayek, S.; Guenther, H.:
Bed shear stress in the southern North Sea as an important driver for suspended sediment dynamics
In: Ocean Dynamics (2008) Springer

DOI: 10.1007/s10236-008-0171-4

Manuscript
Click here to download Manuscript: Stanev_et_al_1_WATT_sp_issue.pdf Click here to view linked References

Emil Vassilev Stanev [1, 2] • Mikhail Dobrynin[1] • Andrey Pleskachevsky [1, 2] • Sebastian Grayek [2]• Heinz Günther [1]

Bed shear stress in the Southern North Sea as an important driver for sediment dynamics

1: Institute for Coastal Research, GKSS Research Centre, Geesthacht, Germany
2: Institute for Chemistry and Biology of the Sea (ICBM), University of Oldenburg, Germany

Submitted to Ocean Dynamics (April, 2008)

Abstract The paper addresses the spatial and temporal patterns of drivers for sediment transport in coastal areas. The focus is put on the bed shear stress in the southern part of North Sea giving the basic control for deposition-sedimentation and resuspension-erosion. The wave-induced bed shear stress is formulated using a model based on the concept that the turbulent kinetic energy associated with surface waves is a function of orbital velocity, the latter depending on the wave height and period, as well as on the water depth. Parameters of surface waves are taken from simulations with the wave spectrum model WAM (WAve Model). Bed shear stress associated with currents is simulated with a 3-D primitive equation model-HAMSOM. Shear stress due to waves and current shear are subjected to EOF-analysis. After revealing the dominating spatial and temporal patterns of wave fields and bed shear stress, we analyze the similarities and differences with the surface concentrations of suspended matter derived from MERIS satellite data. The results show convincingly that the horizontal distribution of sediment can, to a larger extent, be explained by the local shear stress. However, availability of sediment on the bottom (presence or absence of local sources) is quite important in some areas like the Dogger Bank.

Keywords Sediment transport • **w**ind waves • **t**emporal and spatial patterns • suspended matter

1. Introduction

The sedimentary system in the North Sea displays some persistent patterns revealed from remote sensing observations and *in-situ* measurements, which are still not fully explained. It is clear that the major driving forces for Suspended Particulate Mater (SPM) dynamics are due to several forcing: astronomical (tides), atmospheric (wind), open ocean (mean sea level, currents and thermohaline fields) and coastal (fresh water flux and SPM sources). Although some attempts to explain their individual and collective role in the region of our interest (the Southern North Sea) have been carried out (Pleskachevsky et al., 2005; Stanev et al., 2006), there are still no clear and convincing studies quantifying regional driving for SPM dynamics and its possible impact on the spatial patterns. The present study aims to fill this gap using newest information derived from satellite and simple theory. In particular, it sheds more light on the supply and settling of SPM in the North Sea, based on comparison between remote sensing observations and model estimates for local turbulence. This is of utmost importance because the quality of predictions of sedimentary processes in the North Sea depends crucially upon a thorough understanding of physical processes acting in the system.

The present paper does not aim to address the complexity of the entire sedimentary system, but, rather, it focuses on the driving factors. We admit that numerous numerical studies addressing the individual contribution of different properties of forcing on tidal dynamics exist. For instance, Davies and Lawrence (1994) address the influence of wind and wind wave turbulence on tidal currents, Friedrich et al. (1990) address the impact of relative sea-level rise on the evolution of shallow estuaries. However, the major interest of the present study is on temporal and spatial patterns derived from EOF analysis and their relevance to the satellites observations of sediment distribution in the North Sea. The application of this analysis technique to observations and modelling data, which proved to be very useful for the Wadden Sea (Stanev et al., 2007a) is one important motivation for the present study.

The paper is structured as follows. We first describe in Section 2 the basic characteristics of North Sea sedimentary system, followed in Section 3 by the analysis of wave field and bed shear stress. The relevance of the results to the sedimentary system is addressed in Section 4 by comparing the results from bed shear stress analysis with remote sensing images of SPM. The models used are briefly described in the Appendix to this paper.

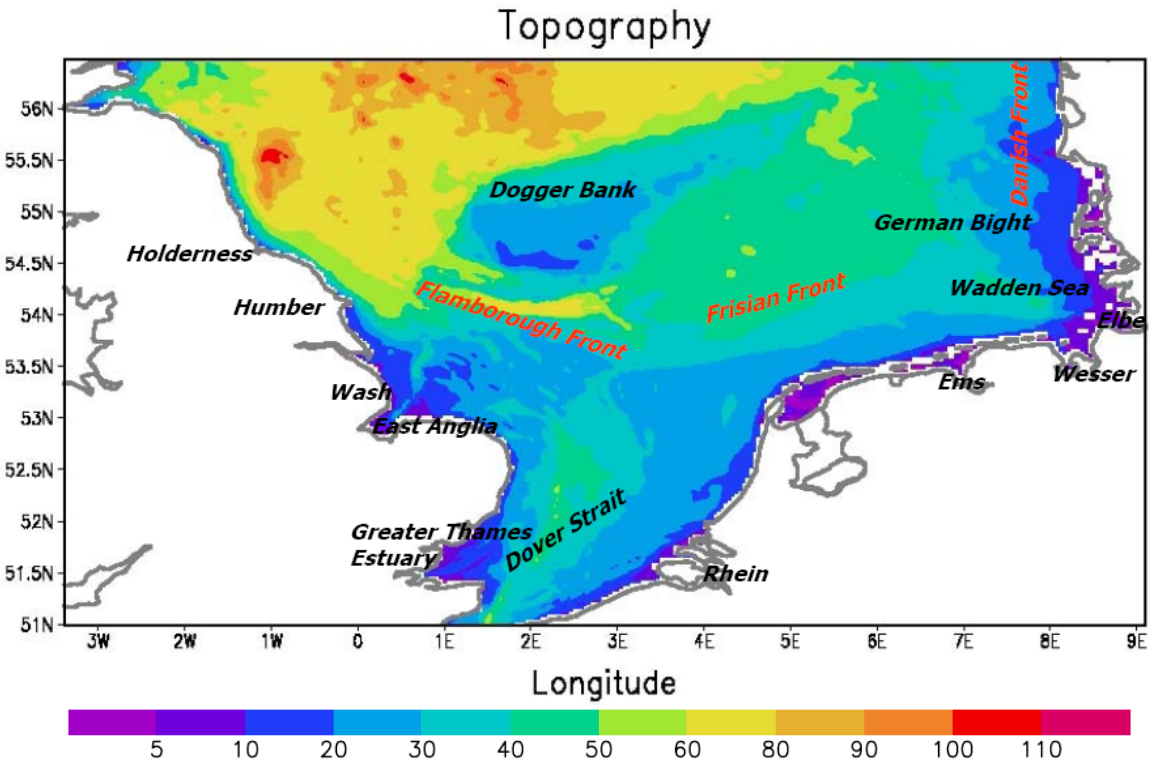

Fig 1. Topography (m) of the Southern North Sea

2. The Southern North Sea Sedimentary system

The major factors explaining the large rate of turbulence in the Southern North Sea are low depths (Fig. 1), strong tides and waves. Local sources from rivers and coast erosion provide a huge amount of suspended matter, which is transported by currents and deposited along some coasts and in the deeper part. The knowledge on spatial patterns of SPM has been limited by the limitation of observations, in particular at the scales of small fronts. For instance, Dyer and Moffat (1998) report an error of 50% in their assessment of suspended matter transport in the East-Anglian plume. Presently, with the availability of ocean colour remote sensing data (e.g., from SeaWiFs, NASA's MODIS sensors and ESA's MERIS sensor) the synoptic mapping of SPM has become a reality (Eleveld et al., 2004; Staneva et al., 2008).

Satellite observations use the fact that absorption and backscatter of seawater depends on concentrations and properties of chlorophyll (CHL), SPM and Coloured Dissolved Organic Matter (CDOM). Ocean colour satellite sensors enable derivation of sediment concentrations from the optical properties of the sea (MERIS Case-2 Regional Processor, Doerffer et al., 2006). Protocols are consistent with REVAMP and MERIS validation protocols (Tilstone and Moore, 2002, Doerffer, 2002). However, remote sensing only provides sediment concentrations over a certain near-surface layer. For the southern North Sea, where stratification is very weak, (dominating vertical homogeneity) concentrations in the near-surface layer differ from the bottom ones mostly due to the specific shape of the sediment profile, which is mostly controlled by turbulence and the settling processes, thus geometrical similarity can be expected between surface and bottom properties.

SPM in the North Sea (Figure 2) originates from fluvial input and is shaped by erosion and resuspension of bottom sediments. An important permanent source in the South is the English Cannel. The residual current in the Dover Strait (about 5 cm/s) fills the Southern North Sea with SPM with concentrations of about 5-10 mg/l. This SPM does not settle there because of strong currents in the Cannel (mean velocity of about 1 m/s). Over large areas in the North Sea, high SPM concentrations are observed in near-coastal areas and over sandbanks with depth less than 20-25 m during calm weather condition. Such areas are Continental, and Scottish-English waters and sometimes the Dogger Bank (in the open sea). In the remaining open sea (North of Dogger Bank) low sediment concentrations of less then 1-2 mg/l occur.

Eleveld et al. (2004), Ruddik (2000) and others proved that SeaWiFS ocean colour sensor covering

the spectrum in 9 narrow optical bands between 400 and 900 nm provides an excellent source for the monitoring of SPM concentrations in the North Sea. They demonstrated that persistent high SPM concentrations are associated with Flemish Banks and the German Bight, and in the Thames Estuary and East-Anglian Plume. In the above areas resuspension is due to turbulence created by current shear (tidal and wind forced). There is evidence that surface waves, especially during strong wind events, provide a key mechanism determining the SPM concentrations in the coastal seas (Gayer et al., 2006).

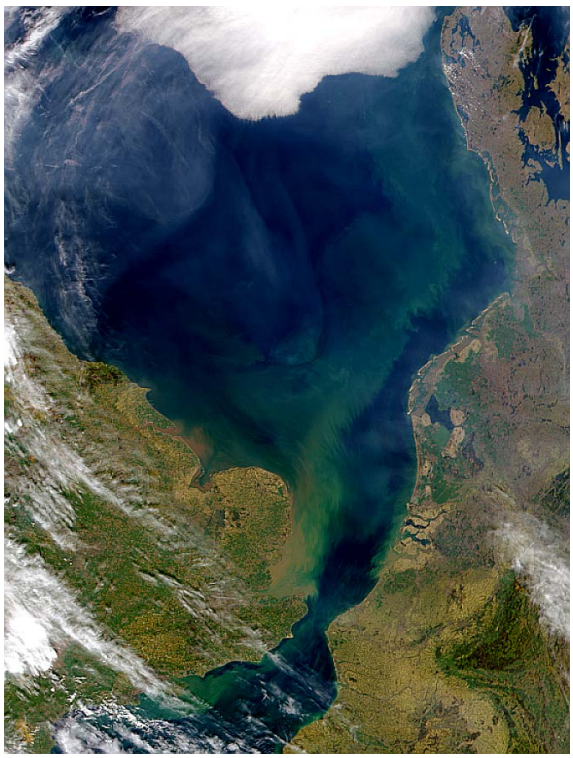

Fig 2. This SeaWiFS image documents the origin and spatial distribution of the sediment pattern being carried into the North Sea. [Source: SeaWiFS Project, NASA/Goddard Space Flight Center, and ORBIMAGE, date: 04-01-1999].

The highest SPM concentrations are usually observed in front of the East-Anglia Coast (Fig. 2) giving an origin of the plume extending in the north-east direction north of Dutch and German coasts (Fig. 1). It is clearly seen in Fig. 2 that this plume, which is called by Dyer and Moffat (1998) as „East-Anglian Plume“ is sometimes „detached“ from the high-concentration zone along the coast. It is usually accepted that the alignment of this plume parallel to the coast is controlled by the along-shore current. However, we will see in this paper, that bottom stress due to surface waves also support such a pattern.

The origin of East-Anglian Plume is associated with the coastal erosion along the coast (Holderness and Norfolk/Suffolk). Another zone of large SPM concentrations is observed along the southern and eastern coast, which is explained by the existence of local sources (rivers) and asymmetries in tidally driven currents promoting the accumulation of sediment (Postma, 1982; Stanev et al., 2007a, b). Waters in the interior sea are clearly separated from coastal waters (Fig. 2) by a system of fronts, some of which are schematically presented in Fig. 1. One observes the lowest concentrations of SPM in the area extending from the Skagerrak (0.4 mg/l) along the Norwegian Trench (0.2 mg/l).

The sediment regime in the German Bight has been addressed in a number of research projects (see Kappenberg and Fanger, 2008 for a review). One such resent activity is the research programme ”BioGeoChemistry of Tidal Flats” (this issue), where observations based on data from in-situ instrumentation, e.g. temperature, salinity sensors and Acoustic Doppler Current Profilers (ADCP), as well as ocean colour sensors onboard satellites, were combined with theoretical studies and numerical modelling aiming to advance the understanding of sediment dynamics in the German Bight and the Wadden Sea, and to provide new estimates for dominating transports. While for some coastal regions, as for instance the German Wadden Sea, the present day knowledge is quite extensive, reaching even analyses on climate and human interventions on the evolution of the Wadden Sea depositional system (Flemming, 2002), for the North Sea in general there is still room to extend the knowledge. This is important for the understanding of the whole system because most of the drivers in near coastal areas are provided by the open sea.

3. Bed shear stress in the North Sea

3.1 Theoretical considerations

Turbulent kinetic energy (TKE) is one of the main drivers of the dynamics of SPM. The complex temporal and spatial patterns of TKE have a number of practical consequences, in particular the physical control of deposition and resuspension/erosion.

An insight about the different levels of TKE due to tides and waves has been provided by Stanev et al. (2006) for the Wadden Sea. Here we focus on the entire Southern part of North Sea. Because the prediction of sedimentary processes in the North Sea depends crucially on a thorough understanding of the individual physical processes acting in the system, we will focus on one of them, which seems to be the most important, that is, the turbulence induced by currents and waves.

Deposition and erosion rates are the major drivers for sediment processes. They are controlled by bed shear stress τ_b which measures the rate of bottom turbulence

$$u^* = \sqrt{\tau_b / \rho}\,, \qquad (1)$$

(remember that close to the bed where the processes are governed by the law of the wall TKE is linearly proportional to the square of friction velocity at the sea floor, u^{*2}). Deposition rate given by Einstein and Krone (1962) is a function of $\frac{\tau_b}{\tau_d}$, where τ_d is the critical shear stress for deposition. The erosion rate given by the formula of Partheniades (1965) is a function of $\frac{\tau_b}{\tau_e}$, where τ_e is the critical shear stress for erosion. Depending on the value of τ_b (compared to τ_d and τ_e) the system is dominated either by deposition or erosion. This motivates us to focus the present study on the bed shear stress τ_b.

Differing from our previous study (Stanev et al., 2006), where the response of sedimentary system to changing magnitude of waves has been addressed using a simple parameterization of wave induced bottom stress (without coupling circulation model with a complex wave model), in this study we analyse the outputs from a wave model and circulation model separately, with a focus on bottom stress. Coupling of a sediment transport model to a wave and circulation model is addressed by Dobrynin et al. (2008).

Bed shear stress is composed of two terms (Grant and Madsen, 1979; Signel, 1990; Davies and Lawrence, 1994):

$$\tau_b = \tau_b^t + \tau_b^w\,, \qquad (2)$$

where the first term is due to tidal dynamics (index "*t*"), and the second one is due to waves (index "*w*"). The contribution of the waves to sediment dynamics can be described using a model that assumes that the turbulent kinetic energy associated with wave-induced bed shear stress is a function of the wave height, wave period (or length) and depth, Pleskachevsky et al. (2005). The parameterization of bed shear stress used in this study is described in Appendix 1.

A similar approach has been used by Davies and Lawrence (1974) to enhance bottom friction in a 3-D numerical model for specific wave periods and magnitudes and by Souza and Simpson (1997) when studying stratification in coastal waters modified by waves.

In order to make further analyses clearer, we will first present in the following some theoretical considerations based on a simpler approach neglecting the wave period, which means the approximation is only valid in water depth less than about one-tenth of the wave length. Bed shear stress is proportional to the second power of the orbital velocity (Jonsson, 1965). Based on this concept, Le Hir et al. (2000) found in the case of shallow water approximation of the orbital velocity (Eq. a6) the following expression

$$\tau_b^w = \frac{\rho \cdot g \cdot fw}{8}\frac{H^2}{h}\,, \qquad (3)$$

where H is the wave height, f_w is the friction factor, and h is the water depth. This equation has been used by Roberts et al. (2000) to study the impact of wave-induced bed shear stress on the equilibrium bottom profile

Assuming a linear relationship between maximum wave height and local depth Eq. 3 is modified by Le Hir et al. (2000) as

$$\tau_b^w = \frac{\rho \cdot g \cdot f_w}{8}\frac{\left[\min\left(H_i, (H/h)_{\lim} h\right)\right]^2}{h}\,, \qquad (4)$$

where $(H/h)_{lim}$ is a limiting value for wave-breaking. For gentle slopes H tends to a constant proportion of the water depth, that is this proportion gives the maximum wave height, that a tidal flat can experience at a given water depth.

This conceptual model suggests that erosion will be enhanced in the depth range where the depth is still large enough to allow high waves (waves with large enough magnitudes, which could substantially affect bed shear stress). Outside of this range (deep-ocean or very shallow depth) either the level of turbulence is low because of the large depths, or the wave height is small because of the small depth.

3.2 Analysis of bed shear stress

Before describing bottom turbulence, we will first briefly analyse the major forcing for the sedimentary system, which is the surface waves. Three-hourly data are subject to EOF analysis (von Storch and Zwiers, 1999). The first three modes of variability (Fig. 3) describe 82.5, 8 and 4.4 percent of the total variability. Principal components are very similar to the ones of bed shear stress and will be addressed later.

The horizontal pattern displayed by the EOF-1 has a maximum in the interior part of the sea, the values having the same sign everywhere. This pattern represents the decrease of significant wave height over the shallows and, due to fetch limitation, along the coast lines. The second and third EOF-s display a rotational structure with the centre at 54.5,N 4E. These dipoles most probably reveal the wave growth with fetch depending on the dominant wind directions. However, most of variability is in the interior part of the basin (EOF-1).

The computation of bed shear stress is explained in detail in Appendix 1. Three-hourly data are subject to EOF analysis. The total variance (Table 1) can be explained by several modes only, in particular for surface waves induced stress.

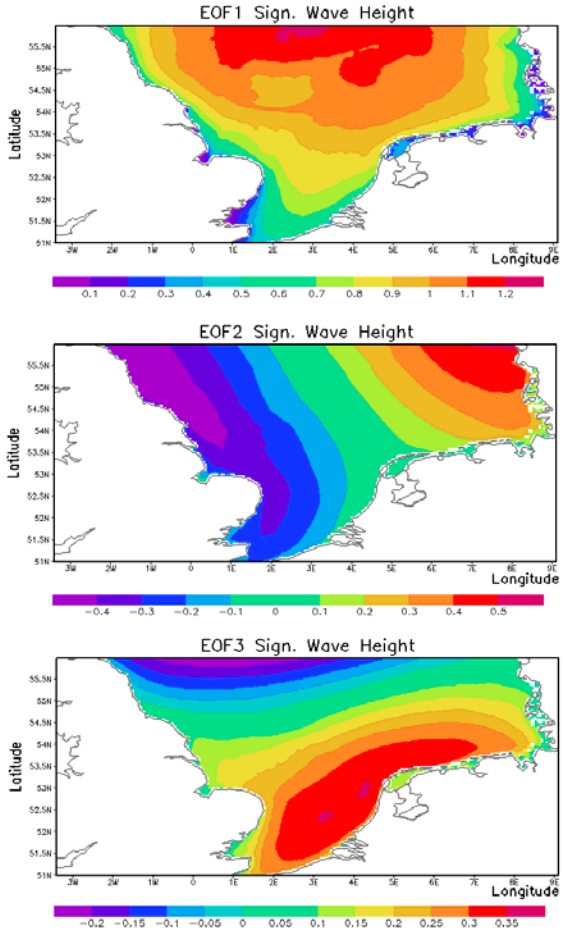

Fig 3. The first three EOF modes of significant wave height

Table 1: Explained variance of bed shear stress by the EOF's computed separately for the waves and current contributions in percent.

EOF-No	waves variance (%)	currents variance (%)
1	77.9	31.2
2	10.0	23.1
3	3.0	16.5
4	1.7	5.9
5	1.4	3.6
Sum	94.0	80.3

Temporal variability is dominated by storminess (Fig. 4a) for surface waves. This curve almost coincides with the „package" of curves for individual locations, the difference is only the magnitude of oscillations. The summer period (May-October) is very quiet.

A persistent weekly cycle dominates bed shear stress due to currents (Fig. 4b). This periodicity is probably a harmonic of the spring-neap cycle. Variability with ~14 day period (spring-neap) can be identified in the associated with currents-PC-s only after the third mode.

Although EOF patterns do not obligatory reveal individual physical processes or controls, their analysis is usually very useful. As seen by the first three EOF-modes (Fig. 5) wave-induced bed shear stress display very rich spatial variability. EOF-1 is positive overall, which means that the dominating response of shear stress to wind waves appears everywhere almost simultaneously.

Largest amplitudes are trapped by shallow depths over most of the area (compare with Fig. 1). However, some deviations from this „rule" are clearly seen in areas which are sheltered by coasts (e. g. Wash and Thames Estuary). These analyses aptly depict small-scale morphological features in front of East-Anglian and Duch-German coasts. EOF-2 and EOF-3 display dynamic features associated with propagation of wind waves. Both EOF-s are bi-polar.

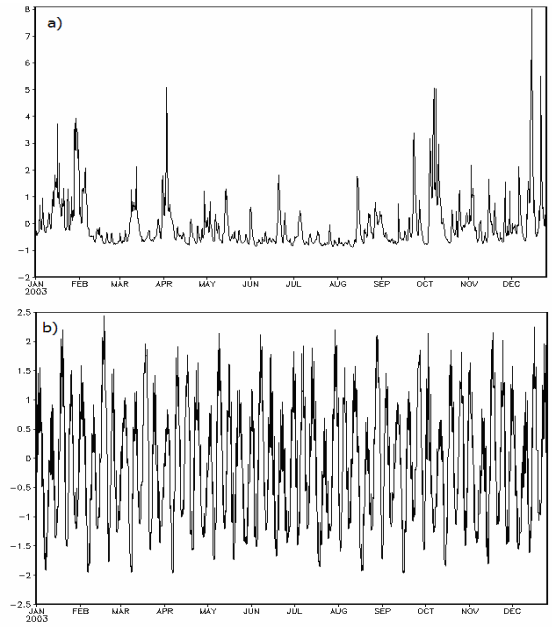

Fig 4. First Principle Components (PC-1) for stress due to waves (a) and currents (b).

In EOF-2 the wave induced bed shear stress along British and German-Danish coasts are inversely correlated. The zero-line (line of minimum amplitude) is in NW-SE direction and divides the southern part of North Sea into two. Analogous structure, but oriented approximately in the East-West direction is noticeable in EOF-3. In this case, the southern coasts and the area north of the line Romo-Wash are negatively correlated. It is noteworthy that the zero line coincides approximately with the northern boundary of Frisian Front, which could justify the speculation that low amplitude oscillation along this line are beneficial for the propagation of SPM-reach water originating from the East-Anglian coast. Both EOF's show basically the same structure as the in the corresponding EOF's of significant wave heights (compare Fig. 5b and c with Fig. 3b and c). Reconstruction of bed stress using only 2-nd and 3-rd modes displays a rotation pattern with wind-wave-„ inverse-amphydrome" at about 54.5,N 4E.

EOF patterns derived from bed stress due to currents (Fig. 6) are quite different from those corresponding to wind waves. All coastal areas

along the British coast are positively correlated in EOF-1, which displays a rapid propagation pattern. Maximum amplitudes are simulated in front of East-Anglia, enhancing the erosion of this area. East-Frisian Wadden Sea is the second most variability-important zone, where turbulence is enhanced by currents. It is interesting that this zone is decoupled from the one off East-Anglia by a small zone with an opposite phase North-West of Texel. Similarly, variability along the western coast is organized in two sub-zones, North and South of Wash.

EOF-2 displays some small-scale patterns, most important of which are the ones East and West of Texel and North and south of Wash. The latter zone is also the major contributor to spatial variability. It provides a clear signal extending in the North-East direction in the area of Frisian Front.

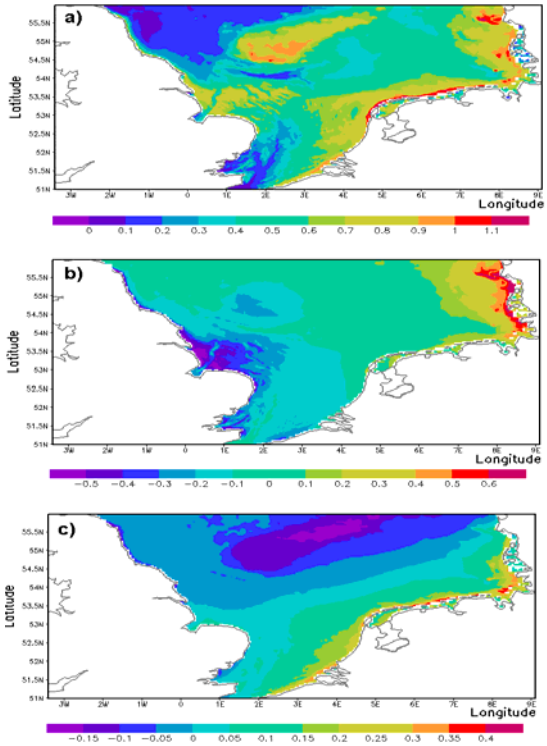

Fig 5. First three EOF modes of shear stress induced by waves.

4. Comparison with remote sensing observations.

Satellite data obtained from MERIS (medium-spectral resolution, imaging spectrometer operating in the solar reflective spectral range) is used for the comparison between the bed shear stress and SPM surface concentrations. MERIS level 1b data was processed using the MERIS Case-2 Regional Processor (Doerffer et al., 2006) to calculate SPM concentrations at the sea surface). For the period of 2003, we analysed approximately 300 MERIS scenes. MERIS scenes shown here were selected in order to cover large parts of the Southern North Sea. Nevertheless, most of them display limited coverage, in particular during winter. This is unfortunate because no complete comparison can be carried out between dynamical forcing (bed shear stress) and the response of the sedimentary system (suspended sediment from satellite) for cases with high waves when the sky is cloudy. We show in Fig. 7 six scenes in chronological order. In the bottom part of each one a curve is plotted showing the variability in the area mean wave height several days before the observation.

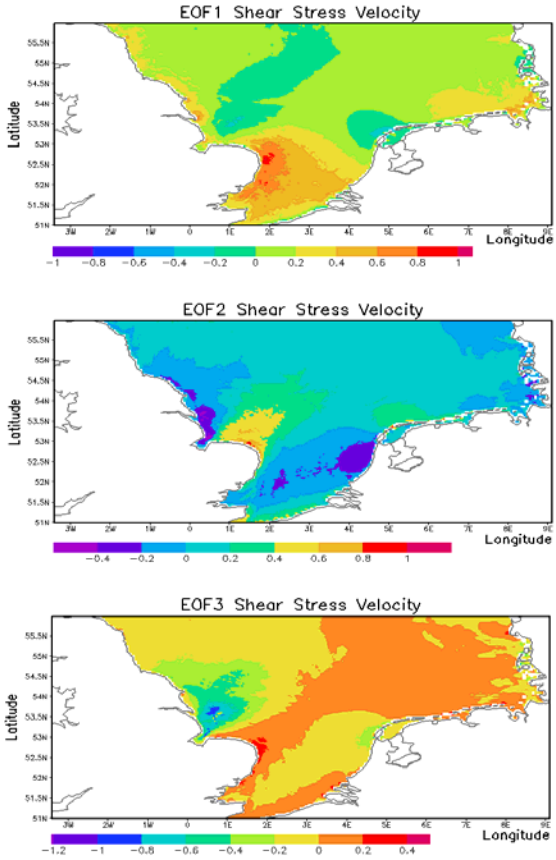

Fig 6. First three EOF modes of shear stress induced by currents.

During very weak (Fig. 7e) and weak (Fig. 7d) wave conditions the SPM concentration is very low over almost the whole area. The areas with high concentrations are squeezed near the river mouths (Humber, Rein, Ems, Weser and Elbe). The signal does not provide enough resolution to resolve East-Anglian Plume, or what is more plausible, this feature is not observed during these times.

The situation during 22 March also corresponds to weak wave conditions (Fig. 7a). This situation was preceded by persistent condition until 13 March when wave height was above 2 m (reaching 3m for a short period). What is seen in Fig. 7a is probably the fate of the East-Anglian Plume one week after the moderate wind conditions. This pattern replicates EOF-1 (Fig. 5) well, in particular along the German coast and off East-Anglia. One striking conclusion however emerges from this comparison: Not all correlations between bed shear stress due to waves and SPM concentration are good. The correlation is especially poor in front of Thames

Estuary and over the Dogger Bank. The „problem“ is partially solved if we refer to EOF-1 of bed shear stress due to currents (Fig. 6). High magnitude of signal north of Thames Estuary, along with the river source, is the obvious explanation of increased SPM concentration seen in MERIS data. The rapid decrease of SPM maximum north of the Rein Estuary could be due to the same shape in EOF-1 in wave-induced bottom turbulence, as well as to the negative correlation in stress due to currents in this area (Fig. 5a).

Figures 7 b, c, and d provide an idea of the temporal evolution of sedimentary state before and after a storm. The front separating Scottish and English coastal waters from open seawaters is very obvious in Fig. 7b. With the increasing wave height (5m on 3rd April), East-Anglian Plume increases in coverage and the patch of increased surface concentrations deviates to the North before reaching the eastern coast. Low sediment concentrations also decouple coastal waters from the plume after the storm. This is another important spatial characteristic of North Sea sedimentary system know from previous observations with different sensors (Eleveld et al., 2004, see also Fig. 2).

It appears clear, that also during storm conditions, no clear correlation exists between Dogger Bank maximum in EOF-1 (Fig. 5a) and SPM concentration. The lack of a correlation could mean that there is no source of sediment in this location. This conclusion is supported by observations (Figge, 1981) and provides a clear indication that care has to be taken in numerical models in order to correctly prescribe availability of sediment on the bottom in order to provide realistic source (Pleskachevsky et al., 2005)

---

4. Conclusions

This study is aimed at making an inventory of dominating SPM patterns in the Southern North Sea and their correlation with bed shear stress. It has demonstrated that the major pattern of wave induced bed shear stress (Fig. 5a) approximately follows the bottom contours (Fig. 1). However, this does not provide an explanation of the increased SPM values in and north of the Thames Estuary. In this area, current-induced bed shear stress seems to provide the major control on resuspension-erosion of sediment. In other areas, such as the Dogger Bank, bed shear stress does not provide an explanation of low values of observed SPM. This gives an indirect support to the evidence that availability of bottom sediment in this area is limited.

This study does not intend to neglect the role of many other important processes (e. g. advection of SPM, Stanev et al., 2007a). Obviously, the real sedimentary system is much more complex. However, it seems that (1) local sources and sinks provide the first order picture about SPM dynamics, (2) they are strongly controlled by turbulence in the bottom layer, and (3) further consideration of parameterizing and prescribing bottom sources is needed to improve quality of bottom boundary conditions used in numerical models.

One further result emerging from this study is the “rotation” of the 2nd and 3rd-mode variability pattern. This model feature is obviously a result of specific “rotation” of the wave height pattern. In order to exclude the suspicion that this feature is simply an artefact of the problems with boundary condition along the northern boundary, we analysed similar results produced with coarse-resolution model for the entire North Atlantic. The mentioned “rotation” in the North Sea was still there demonstrating that this type of variability presents a characteristic form of adjustment of the North Sea wave field to the variability in weather conditions and the fetch, dependent upon wave growth.

Appendix 1. Models used

The bed shear stress components due to currents and waves are calculated using the ocean currents simulated by the HAMburg Shelf Ocean Model (HAMSOM) and waves estimated with the ocean wave spectrum model WAM (WAve Model). Waves are represented by significant wave height, wave period (TM2) and wave direction.
Meteorological forcing for the models HAMSOM and WAM is based on hourly data calculated by the Regional Model of atmosphere (REMO) (Feser et al., 2001). It includes the wind components, atmospheric pressure, air temperature, relative humidity and cloudiness.
The model runs were performed for the year 2003. The region of interest is the southern North Sea from $50.87^{\circ}N$ to $57.17^{\circ}N$ and from $3.40^{\circ}W$ to $9.10^{\circ}E$. Both models were integrated on the same grid with the horizontal resolution of 1.5' in the north-south direction and 2.5' in the east-west direction (corresponding to 2.5-3 km).

HAMSOM model

The three-dimensional ocean circulation model HAMSOM is a baroclinic, primitive equation model described and validated by Backhaus (1985) and Pohlmann (1996). It includes the equations of momentum, continuity, and seawater state, as well as transport equations for temperature and salinity. The model uses a semi-implicit numerical scheme. It is one-way nested into a large-scale HAMSOM model domain for the North Atlantic and uses sea level elevation and climatic averages of temperature

and salinity at the open boundaries. The model has 21 vertical layers variable from 5.0 m in the upper layers and up to 10 m in the lower layers and a time step of 5min. The fresh water sources are represented in the model by the rivers Weser, Ems and Rhein (DOD, 2006), the Ijssel, Nordzeekanaal and Scheldt (Pätsch and Lenhart, 2004), the Thames, Welland, Humber, Tees, Tyne and Forth (GRDC, 2006) and the Elbe, Weser, Ems and Rhine (DOD, 2006). The fresh water discharges data were linearly interpolated to fit the temporal resolution of the model.

WAM model

WAM is a third-generation wave spectral model, which solves the wave transport equation explicitly without any *a priori* assumptions on the shape of the wave energy spectrum. A detailed description of the WAM model is given by Günther et al. (1992) and Komen et al. (1994). WAM is a state-of-the-art spectral wave model specifically designed for global and shelf sea applications. It can run in deep or shallow waters and includes depth and current refraction (steady depth and current field only). It can be set up for any local or global grid with a prescribed data set, and grids may be nested for fine scale applications. The WAM was applied first for the North Atlantic on a coarse grid and then for the southern North Sea (shallow water mode) using the boundary conditions (wave spectra) from the WAM run for the North Atlantic.

Bed shear stress velocity

Bed shear stress velocity u^* (see Eq. 1) is calculated under consideration of local current and waves according to Solsby (1997). The maximum bed shear stress velocity τ_{max} during a wave cycle under vector combining wave and currents is given by:

$$\tau_{max} = \sqrt{(\tau_m + \tau_{wave}\cos\phi)^2 + (\tau_{wave}\sin\phi)^2} \quad \text{(a1)}$$

where ϕ is the angle between current and wave, τ_{wave} is the bed shear stress due to waves, τ_m is mean shear stress given by:

$$\tau_m = \tau_{cur}\left[1 + 1.2\left(\frac{\tau_{wave}}{\tau_{cur} + \tau_{wave}}\right)^{3.2}\right] \quad \text{(a2)}$$

where τ_{cur} is current-only bed shear stress and is related to the depth (lowest water layer) averaged current speed $\overline{U}$ using the drag coefficient C_D by the quadratic friction law

$$\tau_{cur} = \rho \cdot C_D \cdot \overline{U}^2 \quad \text{(a3)}$$

The value of C_D is determined by bed roughness length Z_0 and the thickness of the lowest water layer (water depth by 2D modelling) H_{bod}:

$$C_D = 0{,}16\left(1 + \ln\left(\frac{Z_0}{H_{bod}}\right)\right)^{-2}, \quad \text{(a4)}$$

where $Z_0 = d_{50}/12$, and d_{50} is mean grain size.

The bed shear stress due to waves τ_{wave} uses wave friction factor f_w and the orbital wave velocity at the bottom U_w:

$$\tau_{wave} = \frac{1}{2}\rho \cdot f_w \cdot U_w^2, \quad \text{(a5)}$$

The value of U_w is calculated by

$$U_w = \frac{\pi H_S}{T\sinh(kh)} \quad \text{(a6)}$$

where H_s is significant wave height, T is the wave period (*Tm2* period is used), k is the wave number, h is water depth. The wave friction factor is based on Reynolds number R_w and the relative roughness r:

$$R_w = \frac{U_w A}{\nu}, \quad \text{(a7)}$$

$$r = \frac{A}{k_s}, \quad \text{(a8)}$$

where the Nikuradse roughness length $k_s = 2.5 * d_{50}$, ν is the kinetic viscosity, and the semi-orbital excursion $A = U_w T/2\pi$.

$$f_w = max\{f_{wr}, f_{ws}\}. \quad \text{(a9)}$$

The rough-bed wave friction factor f_{wr} is given by Soulsby:

$$f_{wr} = 0{,}237 r^{-0{,}52} \quad \text{(a10)}$$

The smooth –bed wave friction factor f_{ws} is given by

$$f_{ws} = B \cdot R_w^{-N}, \quad \text{(a11)}$$

where

B=2, N=0,5 for $R_w \le 5\cdot 10^5$ (laminar),
B=0,0521, N=0,187 for $R_w > 5\cdot 10^5$ (turbulent).

As described in Section 3.1 the value of bed shear stress velocity u^* controls the sedimentation and erosion of SPM. In the area of our study, according to Gayer et al. (2006), sedimentation occurs for $u^* < 0{,}0099$ m/s, for $0.010 < u^* < 0.028$ m/s resuspension of SPM occurs, while erosion occurs when $u^* > 0.028$ m/s.

Acknowledgements

This study was supported by DFG project BioGeoChemistry of Tidal Flats, EU-IP ECOOP, and the BMBF/WTZ Project German-Israel: Climate change, wind-wave interaction and anthropogenic impact on coastal processes. Support from the EU IP ECOOP is also acknowledged.

References

Backhaus, J. (1985). A three-dimensional model for the simulation of shelf sea dynamics. *Dtsch Hydrogr Z*, 38:167–187.

Davies A M and Lawrence J (1994) Examining the influence of wind and wind wave turbulence on tidal currents, using a three-dimensional hydrodynamic model including wave-

current interaction. J Phys Oceanogr, 24: 2441-2460.
Dobrynin, M.; Gayer, G.; Pleskachevsky, A. and Günther, H. Modeling the dynamics of suspended particulate matter in the North Sea. Ocean Dynamics, 2008, under review
DOD (2006). German oceanographic data centre, online dataset, www.bsh.de. Technical report.
Doerfer, R., Schiller, H., and Peters, M. (2006). Meris regional case 2 water algorithms (c2r). www.brockmann-consult.de/beam/software
/plugins/merisc2r-1.1.
Doerffer,R., (2002) Protocols for the Validation of MERIS WAter Products, PO-TN-MEL-GS-0043, GKSS, 42 p.
Dyer KR and Soulsby RL (1988) Sand transport on the continental shelf. Annual Review of Fluid Mechanics 20: 295-324.
Einstein HA, Krone RB (1962) Experiments to determine modes of cohesive sediment transport in salt water. J Geoph Res 67: 1451-1461
Eleveld, M.A. & Woerd, H.J. van der (2006). Patterns in water quality products of the North Sea: variogram analyses of single and compound SeaWiFS CHL & SPM grids. In Kerle, N. & Skidmore, A.K. (Eds). Remote Sensing: From Pixels To Processes. ISPRS Proceedings Technical Commission VII. Enschede (The Netherlands): ITC, 93-99.
Eleveld, M.A., Paterkamp, R. & Van der Woerd, H.J.. A survey of total suspended matter in the southern North Sea based on the 2001 SeaWiFS data. EARSeL eProceedings 3, 2/2004
Feser, F., Weisse, R., and von Storch, H. (2001). Multi-decadal atmospheric modeling for europe yields multi-purpose data. *EOS Transactions*, 82 28:345–402.
Figge K (1981) Karte zur Sedimentverteilung im Bereich der Deutschen Bucht im Massstab 1: 250000. Nr. 2900. Deutsches Hydrographisches Institut, Hamburg, Germany
Flemming BW (2002) Effects of climate and human interventions on the evolution of the Wadden Sea depositional system (Southern North Sea).In: Wefer G, Behre K-E, Jansen E. (eds) Climate development and history of the North Atlantic realm. Springer-Verlag Berlin Heidelberg: 399-413.
Friedrichs CT, Aubrey DG, Speer PE (1990) Impact of relative sea-level rise on evolution of shallow estuaries. In: R.T. Cheng (ed.), Residual Currents and Long-Term Transport. Springer-Verlag, New York, pp 105-122.
Gayer, G., Dick, S., Pleskachevsky, A., and Rosenthal , W. (2006). Numericl modeling of suspended matter transport in the North Sea. Ocean Dynamics, 56:62-77.
Grant WD and Madsen OS (1979) Combined wave and current interaction with a rough bottom. J Geophys Res 84: 1797-1808
GRDC (2006). Global runoff data centre, online dataset, http://grdc.bafg.de. Technical report.
Jonsson IG (1966) Wave boundary layers and friction factors. In: Proceedings of the 10-th International Conference on Coastal Engineering, Tokyo, Japan, ASCE, pp. 127-148
Le Hir P, Roberts W, Cacaille O, Christie M, Bassoulet P, Bacher C (2000) Characterization of intertidal flat hydrodynamics. Cont Shelf Res 20: 1433-1459.
Partheniades E (1965) Erosion and deposition of cohesive soils. Journal of the Hydraulic Division, ASCE, 91(HY1)
Pätsch, J. and Lenhart, H.-J. (2004). Daily Loads of Nutrients, Total Alkalinity, Dissolved Inorganic Carbon and Dissolved Organic Carbon of the European continental rivers for the years 1977-2002., page 159. Number 48 in Berichte aus dem Zentrum für Meeres- und Klimaforschung, Reihe B: Ozeanographie.
Pleskachevsky, A., Gayer, G., Horstmann, J., Rosenthal, W. (2005) Synergy of satellite remote sensing and numerical modeling for monitoring of suspended particulate matter. Ocean Dynamic 55 (1): 2-9
Pleskachevsky, A., J. Horstmann, G. Gayer, and W. Rosenthal (2002) Synergy of remote sensing and numerical modelling for suspended matter transport monitoring. In Geoscience and Remote Sensing Symposium, IGARSS apos;02. 2002 IEEE International, Volume 4, Issue , 24-28 June 2002 Page(s): 2397 – 2399.
Pohlmann, T. (1996). Predicting the thermocline in a circulation model of the North Sea. parti: Model description, calibration, and verification. *Cont Shelf Res*, 7:131–146.
Postma, H., 1982. Hydrography of the Wadden sea: movements and properties of water and particulate matter. In: Postma, H. (Ed.), Final Report on 'Hydrography' of the Wadden Sea Working Group—Report 2, Rotterdam, Balkema, 76pp.
Roberts WR, Le Hir P, Whitehouse RJS (2000) Investigation using simple mathematical models of the effect of tidal currents and waves on the profile shape of intertidal mudflats. Cont Shelf Res 20: 1079-1097.
Ruddick K G, F Ovidio & M Rijkeboer, 2000. Atmospheric Correction of SeaWIFS Imagery for for Turbid Coastal and Inland Waters. Applied Optics, 39(6): 897-912
Signell RP, Beardsley RC, Graber HC, and Capotondi A (1990) Effect of wave-current interaction on wind-driven circulation in narrow, shallow embayments. J Geophys Res 95: 9671-9678.
Souza AJ and Simpson JH (1997) Controls on stratification in the Rhine ROFI system. Journal of Marine Systems, 12: 311-323.
Stanev EV, G Brink-Spalink J-O Wolff (2007a) Control of sediment dynamics by transport and turbulence. A case study for the East Frisian Wadden Sea. J Geoph Res. Vol. 112, C04018, doi:10.1029/2005JC003045
Stanev, E. V., B. W. Flemming, A. Bartholoma¨, J. V. Staneva, and J.-O. Wolff (2007b), Vertical circulation in shallow tidal inlets and back-barrier basins, Cont. Shelf Res., 27, 798– 831, doi:10.1016/j.csr.2006.11.019.
Stanev, E. V., J. O. Wolff, and G. Brink-Spalink (2006) On the sensitivity of sedimentary system in the East Frisian Wadden Sea to sea level rise and magnitude of wind waves. Ocean Dynamics 56(3-4): 266-283 ISSN 1616-7341
Staneva, J., E. V. Stanev, J.- -O. Wolff, T. Badewien, R. Reuter, B. Flemming, A. Bartholom¨a, and K. Bolding (2008) Hydroynamics and Sediment Dynamics in the German Bight. A Focus on Observations and Numerical Modelling in the East Frisian Wadden Sea. Cont. Shelf Res., (in press).

Van der Woerd H & R Pasterkamp. Mapping of the North Sea turbid coastal waters using SeaWiFS data. Canadian Journal of Remote Sensing, 30(1): 44-53
Van Raaphorst W, C J M Philippart, J P C Smit, F J Dijkstra, & J F P Malschaert, 1998.Distribution of suspended particulate matter in the North Sea as inferred from NOAA/AVHRR reflectance images and in situ observations. Journal of Sea Research, 39: 197-215
von Storch, H., Zwiers, F.W., 1999. Statistical analysis in climate research. Cambrigde University Press, 494 pp.

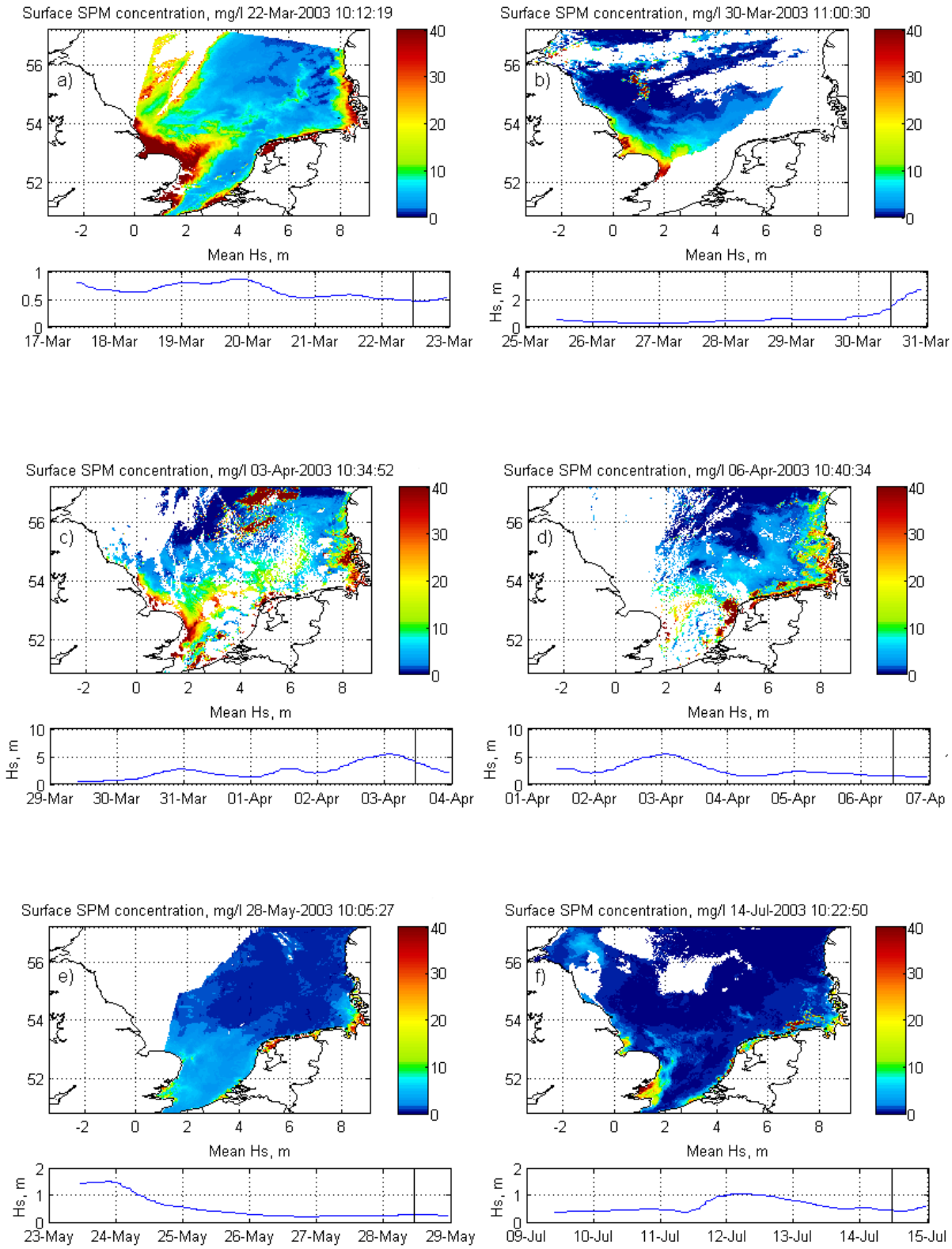

Fig 7. Suspended sediment concentration obtained from MERIS data for 22 March (a), 30 March (b), 03 April (c), 06 April (d), 28 May (e), and 14 July (f). Bottom part of each panel gives area mean significant wave height during the last five days before the scene.